physica status solidi pss b
www.pss-b.com
basic solid state physics

Prediction of size disorder induced resonant tunneling in large scale nanodot arrays

J. Chen, J. J. Lu, and **W. Z. Shen**

Laboratory of Condensed Matter Spectroscopy and Opto-Electronic Physics, Department of Physics, Shanghai Jiao Tong University, 1954 Hua Shan Road, Shanghai 200030, P.R. China

Received 12 April 2006, revised 28 July 2006, accepted 14 August 2006
Published online 27 September 2006

PACS 05.60.Gg, 73.23.Hk, 73.63.Kv

We have successfully investigated the effect of size fluctuation on the resonant tunneling characteristics of nanodots arrays. The approach was realized with taking into account the induced electron energy level disorder under the framework of the generalized Breit–Wigner formula. It is found that the dot size fluctuation has played an important role in both the tunneling current profile and number of the resonant peaks. By the aid of the statistical concept to characterize the size fluctuation in large scale nanodots systems, we have shown a clear picture for the dependence of the resonant peak number and peak to valley ratio on the degree of disorder and spatial configuration in the nanodots. The whole investigation will give a general prediction of the origin of resonant tunneling phenomena observed in large scale nanodot systems.

phys. stat. sol. (b) **244**, No. 2, 587–595 (2007) / **DOI** 10.1002/pssb.200642178

Original Paper

phys. stat. sol. (b) **244**, No. 2, 587–595 (2007) / **DOI** 10.1002/pssb.200642178

Prediction of size disorder induced resonant tunneling in large scale nanodot arrays

J. Chen[*], **J. J. Lu,** and **W. Z. Shen**

Laboratory of Condensed Matter Spectroscopy and Opto-Electronic Physics, Department of Physics, Shanghai Jiao Tong University, 1954 Hua Shan Road, Shanghai 200030, P.R. China

Received 12 April 2006, revised 28 July 2006, accepted 14 August 2006
Published online 27 September 2006

PACS 05.60.Gg, 73.23.Hk, 73.63.Kv

We have successfully investigated the effect of size fluctuation on the resonant tunneling characteristics of nanodots arrays. The approach was realized with taking into account the induced electron energy level disorder under the framework of the generalized Breit–Wigner formula. It is found that the dot size fluctuation has played an important role in both the tunneling current profile and number of the resonant peaks. By the aid of the statistical concept to characterize the size fluctuation in large scale nanodots systems, we have shown a clear picture for the dependence of the resonant peak number and peak to valley ratio on the degree of disorder and spatial configuration in the nanodots. The whole investigation will give a general prediction of the origin of resonant tunneling phenomena observed in large scale nanodot systems.

1 Introduction

Transport properties of nanodots have received an increasing attention in recent years, among which resonant tunneling is of particular interest both from the physics viewpoint and with regard to its application in the nanoelectronics. The principal feature of the resonant tunneling is the existence of resonant peaks in current–voltage (I–V) characteristics, which has been intensively experimentally observed [1–6] and theoretically studied [7–10]. For the simplest single or double dots case, the resonant tunneling occurs when the electron levels in one dot are aligned to those in the electrode or the other dot. Therefore, the number of electron energy levels in the dots is usually reflected by the number of the resonant peaks in I–V curves.

With the progress of fabrication techniques, well-arranged complicated nanodots structures have been synthesized within the reach of experimental investigation [11–14], such as chains [11] and rings [13], which usually contain a certain number of nanodots. However, larger scale system will induce more disorder mechanisms into it and the experimental I–V characteristics usually reveal more complicated features than single or double dots cases. These extra current peaks in the I–V curve may be influenced by various origins of disorders, which have become an active field of research in the past decade [3, 15–18]. Among all the studied disorder mechanisms, the energy level disorder in dots plays the most important role since the nonaligned energy level in two adjacent dots will cause the accumulation and release of electrons at different applied voltage, which will significantly change the I–V curve. Moreover, although today's advanced nanostructure techniques can provide a good control on the size of nanodots, the size fluctuation in nanodots system is still inevitable [12, 19–21] and a normal distribution of dot sizes is most likely to be formed. Therefore, a detailed theoretical analysis of the resonant tunneling

[*] Corresponding author: e-mail: bageqh@sjtu.edu.cn

induced by the dot size fluctuation is helpful for a better understanding of the resonant tunneling information of the electron levels in those large scale complicated nanodots arrays.

Though many theoretical methods have been developed to investigate the resonant tunneling in nanodots [7–10, 17, 22, 23], most of them, such as the density matrix approach [7], Green's function theory [9], and quantum shuttle approach [17], are too complex to take the size fluctuation into account, especially when the array dimension grows large. Recently, fluctuations of the energy levels (due to fluctuations of the quantum dot sizes) and their combination with Coulomb interaction and Coulomb blocking have been treated, and inhomogeneous quantum dot ensembles have been shown to play a crucial role in explaining the single-peak structures of the current–voltage characteristics [24, 25]. In our paper, we employ a straightforward model generated from generalized Breit–Wigner formula, together with the semiclassical techniques based on the existence of the most probable tunneling paths coupling electrodes and nanodots [10, 26] to accomplish our simulation. This model does not concentrate on a certain material, thus the conclusion we draw would be general and predictive to whatever kind of nanodot material we use. Moreover, it is easy for us to take the normal distribution disorder into consideration. With the help of the model, we have successfully accessed the effects of the size fluctuation on the resonant tunneling characteristics in nanodots arrays. It is found that the dot size fluctuation will have great influence on both the profile of the current curves and the number of the resonant peaks. We have further shown that these alterations are closely related with the configuration of the dots arrays in large scale systems.

2 Results and discussion

In order to illuminate the size fluctuation effects specifically, we consider a resonant tunneling structure of N nanodots between two electrodes with only the ground state in each dot. We suppose that all the resonant levels of the nanodots structure are lower than the Fermi level in the left lead (μ_{L}) and higher than that in the right lead (μ_{R}), thus the electron Fermi-distribution in the metal leads could be neglected. We also assume that the voltage bias is sufficiently high so that the energy change during the tunneling of an electron between a reservoir and the structure is much larger than the energy uncertainty. In this situation the Büttiker equation [27] for the tunneling current has the simplest form of

$$I_T = \frac{e}{\pi\hbar}\int_{-\infty}^{\infty} T(E)\,\mathrm{d}E\,, \tag{1}$$

where the integration is performed over the energies of incident electrons. $T(E)$ is the transmission coefficients between two electrodes.

The transmission coefficients $T(E)$ between two electrodes can be defined by the generalized Breit–Wigner formula [26]:

$$T(E) = \mathrm{Tr}\,(\Gamma_{\mathrm{L}} H \Gamma_{\mathrm{R}} H^{+})\,, \tag{2}$$

where

$$H = (EI - Q - \tfrac{1}{2}\,i\Gamma)^{-1}\,, \tag{3}$$

$$\Gamma = \Gamma_{\mathrm{L}} + \Gamma_{\mathrm{R}}\,, \tag{4}$$

$$\Gamma_{\mathrm{L(R)}} = \begin{vmatrix} \Gamma_1^{\mathrm{L(R)}} & 0 & \dots & 0 \\ 0 & \Gamma_2^{\mathrm{L(R)}} & \dots & 0 \\ \vdots & \vdots & & \vdots \\ 0 & 0 & \dots & \Gamma_N^{\mathrm{L(R)}} \end{vmatrix}, \tag{5}$$

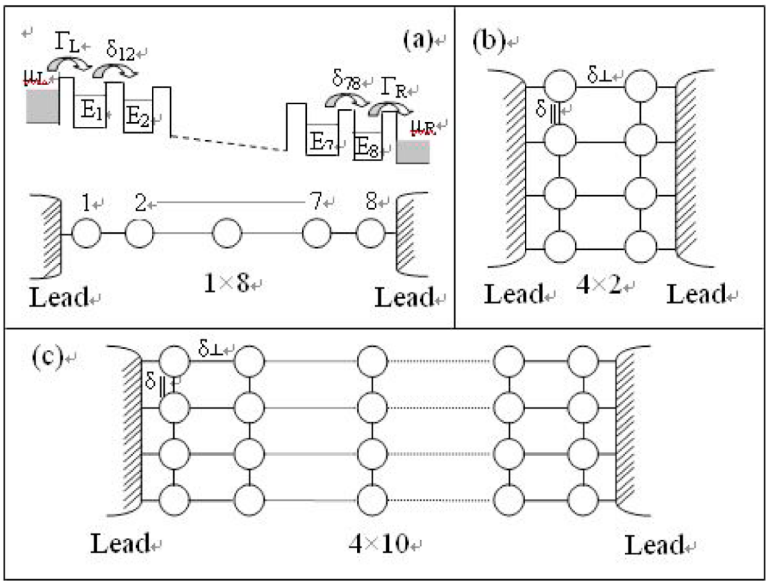

Fig. 1 Nanodots structures: (a) single array (chain) of 1 × 8, together with the sketch of energy diagrams along the paths connecting two leads, multiple arrays of (b) 4 × 2 and (c) 4 × 10 with two leads.

$$Q = \begin{vmatrix} E_1 & \delta_{12} & \dots & \delta_{1N} \\ \delta_{21} & E_2 & \dots & \delta_{2N} \\ \vdots & \vdots & & \vdots \\ \delta_{N1} & \delta_{N2} & \dots & E_N \end{vmatrix}. \tag{6}$$

Here I is the unit matrix, $\Gamma_j^{\mathrm{L(R)}}$ is the partial width of decay from the state in the left (L) electrode into dot j or from the state in dot j into the right (R) electrode, respectively. If the dot (j) does not directly couple with the leads, the value of $\Gamma_j^{\mathrm{L(R)}}$ will be set as zero. The nondiagonal elements of the energy matrix δjk are the flux overlap integrals between eigenstates of dots j and k.

We start with an interesting nanodots chain structure (linear array) [Fig. 1(a)], since the tunnel coupling exists merely between neighboring dots and only the first and the last dots of the array are connected to the electrodes. Moreover, there is one unique path for the current, and changes in any dot will affect the transport through the whole chain. We have also plotted in Fig. 1(a) the sketch of energy diagram of the dots chain, together with the corresponding symbols that designated in our model. For simplicity, all the flux overlap integrals δ_{jk} ($j = 1 \ldots N$, $k = j + 1$ or $j - 1$) are set to be the same value of δ_0 and $\Gamma_\mathrm{L} = \Gamma_\mathrm{R} = \Gamma_0$. The applied voltage V adds to the array as a Stark ladder: $E_i = E_i^0 - i \times V/N$ ($i = 1 \ldots N$) (E_i^0 is the energy level in the dot without bias, and in most reported theoretical calculations, all the E_i^0 are set to be the same, i.e., at energy origin, under the uniform assumption). Figure 2(a) and (b) plot the calculated normalized resonant currents in a uniform eight nanodots chain, where we have taken different Γ_0 values at certain $\delta_0 = t$ (t is a constant of 20 meV) in Fig. 2(a), and changed δ_0 with fixed $\Gamma_0 = t$ in Fig. 2(b). It is clear that the observed typical half Lorentzian profiles are similar to the other previously reported results by the density matrix approach [7]. We note that the current profiles are influenced by both Γ_0 and δ_0: as increasing Γ_0 (δ_0), the width of the $I_\mathrm{T}/I_\mathrm{Tmax}$ Lorentzian curve becomes wider. However, the I–V curve is obviously more sensitive to δ_0 than that of Γ_0. As a result, we have set the value of Γ_0 equal to t in the following calculations since it has no explicit impacts on the tunneling results.

The size fluctuation in the nonuniform nanodots chain will directly lead to the electron level disorder, indicating that the employed eight E_i^0 values are different to each other in the model; however, compared

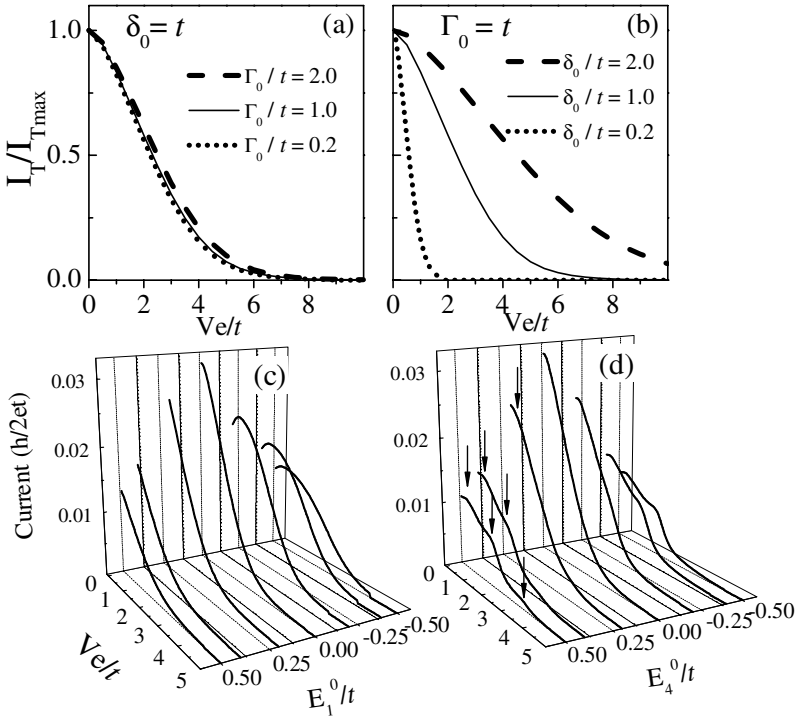

Fig. 2 Normalized resonant current calculated without considering the size fluctuation in the nanodots chain for cases of (a) $\delta_0 = t$, Γ_0 changes and (b) $\Gamma_0 = t$, δ_0 changes. I–V characteristics in the individual nonuniform nanodots chain with the electron level in (c) 1st and (d) 4th dot changing from $-0.5t$ to $0.5t$, respectively. The arrows in (d) are the indication of the resonant peaks.

with the barrier heights, those fluctuations should be smaller. If the size of only one dot (j) in the chain changes, then the energy level E_j^0 inside this particular dot will be higher or lower than that in other dots.

In order to identify the role of a certain dot in the dots chain, we set a number designation for all the dots as 1 to 8 from left to right [shown in Fig. 1(a)]. The electron levels $E_i^0\,(i \neq j)$ in unchanged dots are chosen to be the zero energy point, so that E_j^0 itself is the measure of the energy deviation, which may be either positive or negative. Figure 2(c) presents the dependence of the I–V characteristics on E_1^0, which changes in the range of $-0.5t \sim 0.5t$. The intensity of the current is found to reduce as increasing $|E_1^0|$. If E_1^0 is positive, the I–V curves are similar to the uniform case ($E_1^0 = 0$), and the position of I_{Tmax} is always at zero voltage, except for the narrower profile. In contrast, when E_1^0 is negative, the I–V curves become broader, and the I_{Tmax} moves away from zero voltage. This is because the negative E_1^0 breaks the resonant condition at zero voltage, while increasing forward voltage will lower the levels in the other dots, leading to the occurrence of resonant tunneling. The more negative value E_1^0 gets, the larger voltage is needed for the resonant tunneling. However, no additional resonant peaks can be observed when the electron level in the 1st dot $|E_1^0|$ becomes larger. Figure 2(d) displays the effects of the size fluctuation in the 4th dot (near the center of the whole chain) on the current. It is clear that obvious resonant tunneling phenomena can be observed no matter negative or positive E_4^0 is, and the number of the resonance peaks (marked by arrows) increases with $|E_4^0|$, demonstrating that the fluctuated value of $|E_4^0|$ will significantly alter the tunneling characteristics of the nanodots chain system.

The dependence of the disorder-induced resonant tunneling properties on the position of the individual nonuniform dot has been compared by imposing a same E_j^0 on dot 1–8, respectively. In Fig. 3(a–d) we plot the I–V characteristics (the solid curves) when E_j^0 is acted upon dot 1–4. Actually, the chain configuration symmetry implies that the results on dot 5–8 are similar to those in dot 4–1, respectively, but

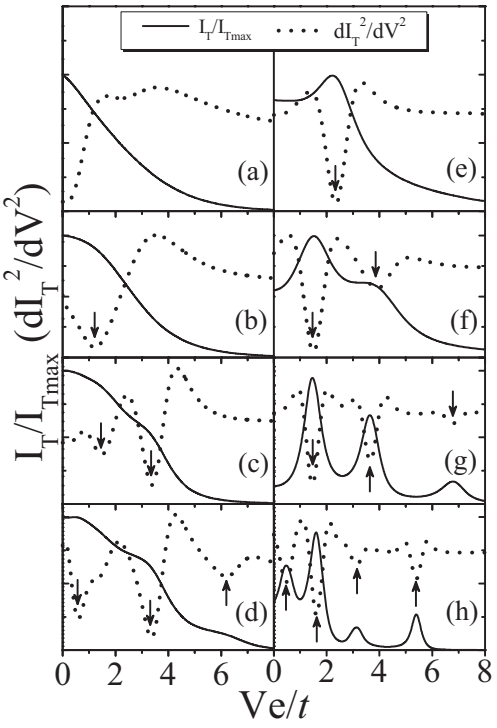

Fig. 3 Dependence of the normalized I–V characteristics on the configuration of the individual nonuniform (a) 1st, (b) 2nd, (c) 3rd, and (d) 4th dot. Dependence of the normalized I–V characteristics on the degree of the randomly fluctuated nanodots chain with different variances σ^2 in the normal distribution: (e) 1×10^{-5}, (f) 5×10^{-5}, (g) 1×10^{-4}, and (h) 2×10^{-4} eV^2. The dotted curves are the second derivative of the tunneling current vs. voltage.

attention should be paid that E_j^0 has to be replaced by $-E_j^0$. From Fig. 3(a–d), we can observe the gradual appearance of the current structures, accompanied by a pronounced background current. The second derivative of the current–voltage characteristics (the dotted curves) reveals clearly the resonance current peaks (marked by arrows) in the nanodots chain. One can intuitively conclude that the disorder in the relative middle position of the chain has more impacts on the I–V characteristics than that in the chain edge. Having analyzed the effect of single one dot fluctuation on the whole I–V properties, we will further discuss the case when the sizes of all the dots are randomly fluctuated in the nanodots chain. In order to obtain a semiquantitative result, all the eight energy levels are presumed to satisfy a normal distribution of:

$$f(E_i^0) = 1/\sqrt{2\pi\sigma}\, \exp[-(E_i^0)^2/2\sigma^2]. \tag{7}$$

Although this kind of statistic assumption may not be suitable for small number dots, we just use it for reference to obtain the dependence tendency on the degree of disorder. Figure 3(e–h) shows the I–V curves with the electron levels generated from different normal distributions in the order of increasing variance σ^2, which is supposed to represent the degree of the electron level disorder, and could reflect the size nonuniformity in dots. Compared with I–V curves induced by the single one dot fluctuation in Fig. 3(a–d), sharper peaks are observed and the number of the resonant peaks increases. Extra current resonant peaks due to the disorder have also been reported in quantum dots chains [17]. Nevertheless, it is interesting to find that the maximum number of the resonant peaks cannot be larger than $N/2$ (N is the total number of dots). This could be attributed to the uniform electron field assumption in our calculation, if the electron field distribution is nonuniform, more peaks may appear because of the field domain effect [28].

Next we turn to the multiple array structures, of which up to now the resonant tunneling characteristics have been reported are in simple cases, such as 2×2, together with a rough discussion about the disorder effects [15]. In our present work, we first deal with a small 4×2 dots array plotted in Fig. 1(b), where four dots are connected to the left electrode while the other four are linked to the right electrode. The flux

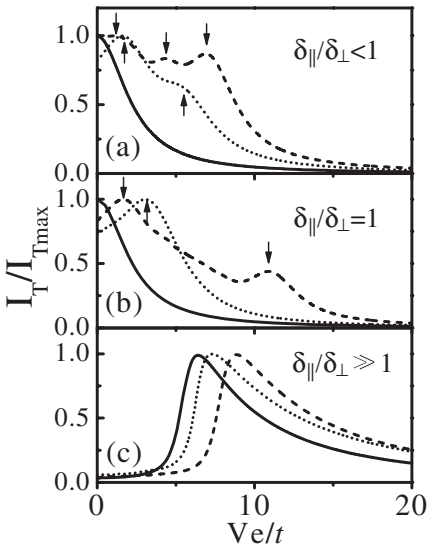

Fig. 4 Normalized I–V characteristics for a 4 × 2 nanodots array under cases of (a) $\delta_{\parallel}/\delta_{\perp} < 1$, (b) $\delta_{\parallel}/\delta_{\perp} = 1$, and (c) $\delta_{\parallel}/\delta_{\perp} \gg 1$. Solid curves: uniform nanodots array. Dotted and dashed curves: nonuniform nanodots array with σ^2 of 1×10^{-4} and 2×10^{-4} eV^2, respectively.

overlap integrals δ_{jk} between neighboring dots can be categorized into two types: $\delta_{\perp}$ and $\delta_{\parallel}$, which denote the perpendicular and parallel relationship to the leads, respectively. According to the ratio of $\delta_{\parallel}/\delta_{\perp}$, the whole issue is divided into three cases: (i) $\delta_{\parallel}/\delta_{\perp} < 1$, (ii) $\delta_{\parallel}/\delta_{\perp} = 1$, and (iii) $\delta_{\parallel}/\delta_{\perp} \gg 1$. The solid curves in Fig. 4 are the calculated I–V characteristics for all the three cases without considering the electron level disorder. There is no obvious difference between the results in cases (i) and (ii) and those in the nanodots chain of Fig. 2. However, we can observe one dominant resonant peak in the case (iii) with $\delta_{\parallel}/\delta_{\perp}$ more than 80, similar to the miniband tunneling phenomenon in superlattice structures [28]. The reason can be attributed to the large $\delta_{\parallel}$ values, where the electrons have been delocalized along this direction and the 3D quantum confinement is turned into 1D confinement.

When taking into account the energy level disorder, the I–V characteristics in these three cases vary differently, where we still use the variance parameter in the normal distribution to represent the degree of disorder in the nanodots array. The dotted curves and dashed curves in Fig. 4 are the calculated results with the variance of $\sigma^2 = 1 \times 10^{-4}$ and 2×10^{-4} eV^2, respectively. Extra resonant tunneling peaks are observed for the cases (i) and (ii), and the number of peaks increases with the variance σ^2 for both two cases, whereas for the case (iii), no obvious change is found, except for a shift of the peak position. In addition, more resonant structures have been revealed in the case (i) than those in the case (ii) by comparing Fig. 4(a) with (b). The above results are understandable. The smaller ratio of $\delta_{\parallel}/\delta_{\perp}$ in the case (i) implies the weaker interaction between nanodots parallel to the lead, which blocks the electrons in one dot from tunneling into another along this direction. In this condition, the 4 × 2 nanodots array eventually evolves into four isolated chains of two dots. For a specific electron injected from the left lead, it has only one way to arrive at the right lead through a specific path, so that the extra resonant peaks are formed by the contribution of four parallel chains. In other words, all the dots in the array will play their roles in the resonance. As for case (iii), the large ratio of $\delta_{\parallel}/\delta_{\perp}$ ensures that the electrons in the dots along the parallel direction can tunnel back and forth freely. After applying the voltage, even if the energy level does not align in one path, electrons can choose another channel that has the least resistance to go through. As a result, the injected electrons do not have the unique way to pass through to the right lead, which can well explain the observation that the nonuniformity in case (iii) does not strongly influence the I–V characteristics.

We then focus on a relatively large scale 4 × 10 nanodots array with the configuration shown in Fig. 1(c), where four parallel chains made of ten dots are perpendicular to the leads. Such large scale nanodots system has been carefully investigated by G. Kießlich et al. and the fluctuations of the energy levels is found to play a crucial role in explaining the single-peak structures of the current–voltage char-

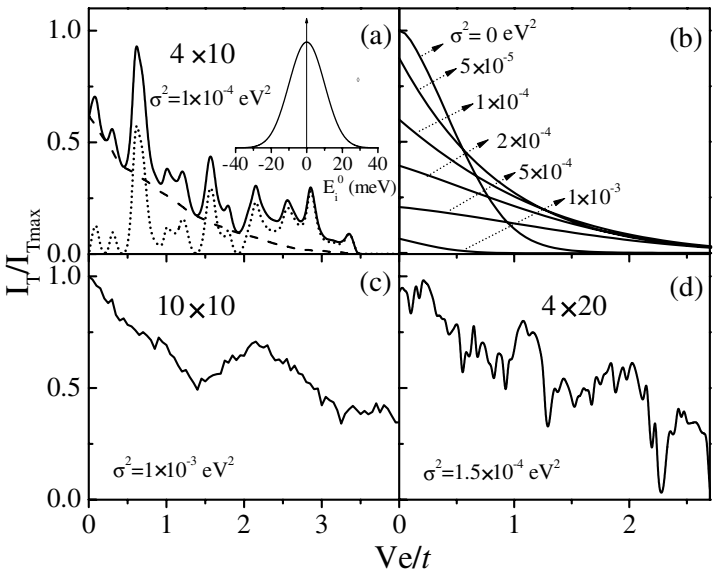

Fig. 5 Normalized I–V characteristics for (a) 4 × 10 nanodots array with $\sigma^2 = 1 \times 10^{-4}$ eV^2, (c) 10 × 10 nanodots array with $\sigma^2 = 1 \times 10^{-3}$ eV^2, and (d) 4 × 20 nanodots array with $\sigma^2 = 1.5 \times 10^{-4}$ eV^2. The dashed and dotted curves in (a) represent the ordering and disordering currents, respectively, with the extracted ordering current at different degrees of disorder shown in (b). The inset in (a) is the electron level normal distribution under $\sigma^2 = 1 \times 10^{-4}$ eV^2.

acteristics [24, 25]. In our simulation, the values of $\delta_{\parallel}$ and $\delta_{\perp}$, as well as $\Gamma_j^{\mathrm{L(R)}}$ are all set to t. The I–V profile without considering the size fluctuation for this system is similar to that revealed in the above 1 × 8 nanodots chain and 4 × 2 nanodots array. With the employment of normal distribution for the disorder, σ^2 of 1×10^{-4} eV^2 corresponds to a 99.97% of the electron levels supposed to fluctuate normally within the range of $-30 \sim +30$ meV [see the inset of Fig. 5(a)]. Figure 5(a) displays the calculated I–V curve with $\sigma^2 = 1 \times 10^{-4}$ eV^2 (solid curve), where eleven resonant peaks are observed with different peak intensities.

After calculating the I–V characteristics with various variances σ^2, we notice that the I–V curves are made up by the overall contribution of both the background current and resonant current, which can be separated by the dashed and dotted curves in Fig. 5(a), respectively. We note that the profile of the extracted background current is quite similar to that in the uniform cases. Furthermore, the intensity of the background current is found to decrease as increasing the variance value and vanishes when σ^2 is larger than 1×10^{-3} eV^2 [see Fig. 5(b)]. These arguments demonstrate that the background current is the reflection of the degree of ordering in the nanodots system, thereby we may define the background current as ordering current.

Alternatively, the resonant current component of the I–V curve is due to the disorder of the nanodots systems, which could be considered as disordering current. Using the normal distribution with the same variance and average values, we calculate the I–V curves for a number of times, which serves as a sampling process, and the simulation results show that the number of the resonant peaks is within a certain range, although the shape of the disordering current may vary every time. For example, when $\sigma^2 = 1 \times 10^{-4}$ eV^2, 20 times of calculations illuminate that the number of the peaks is in the range of 10–12. Figure 6 plots the relationship between the number of the resonant peaks and the variance value σ^2. A maximum resonant peak number is found to occur when σ^2 is around 2×10^{-4} eV^2, while either increasing or decreasing σ^2 from 2×10^{-4} eV^2 will reduce the peak number. This phenomenon can be explained as follows. On the one hand, no resonant peak is produced at certain applied voltage when the size fluctuation does not exist. On the other hand, when the disorder is relatively large, the resonant peak

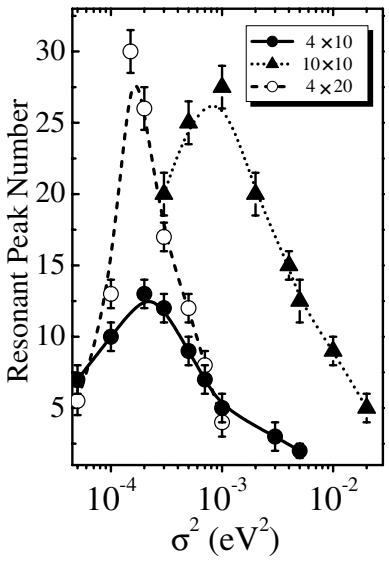

Fig. 6 Relationship between the number of resonant peaks and disorder degree at nanodots arrays of 4 × 10, 10 × 10, and 4 × 20. The curves are guides for eyes.

is also hard to be observed because the electronic levels are difficult to align with each other. Actually, both of the ordering and disordering current will vanish when the fluctuation becomes large enough.

We have further investigated the I–V characteristics of 10 × 10 and 4 × 20 nanodots configurations, shown in Fig. 5(c) and (d), where more resonant peaks appear, whereas the corresponding variance σ^2 to the maximum peak number is quite different. Figure 6 also shows the dependence of the resonant peak number on variance in these two nanodots array configurations, with the maximum peak number at $\sigma^2 = 1 \times 10^{-3}$ eV^2 for the 10 × 10 array and $\sigma^2 = 1.5 \times 10^{-4}$ eV^2 for the 4 × 20 case. Moreover, it is clear that the dependence of the peak number on variance changes more rapidly in the 4 × 20 system, indicating the more significant impact on the I–V curve induced by the dots along the current direction perpendicular to the leads.

Finally, we discuss the peak to valley ratio of the disordering current in the nanodots arrays with different configurations. Comparing Fig. 5(c) and (d) with 5(a), although the number of resonant peaks increases for both of the 10 × 10 and 4 × 20 cases, we find that the peak to valley ratio in the 10 × 10 structure reveals evidently smaller than that in the 4 × 20 and 4 × 10 ones. This phenomenon can be well explained from the array configuration point of view. The 4 × 10 dots system can be considered as four parallel linear (1 × 10) arrays, and the increase of the parallel chains from 4 to 10 (the 10 × 10 case) indicates that more parallel connections are available. The fluctuation in dot size will cause the peaks contributed from different parallel chains deviate from chain to chain, and some of the peaks in one chain may be weakened or counteracted by additional peaks from another chain. Thus, the superimposed current [Fig. 5(c)] displays more resonant peaks for the 10 × 10 nanodots array at the expense of smaller peak to valley ratio. For the 4 × 20 nanodots array, the increase of the dot number in each chain will also result in more disordering current peaks along with narrower peak width. However, since the number of the parallel chains keeps unchanged, no additional deviation induced by extra chains will be presented to decrease the peak to valley ratio in the 4 × 20 system [see Fig. 5(d)]. Therefore, the requirement of high peak to valley ratio in nanoelectronic devices [29, 30] demands more precise control of dot size uniformity in large "parallel connection" nanodots systems.

3 Conclusion

In summary, we have employed the generalized Breit–Wigner formula to deal with the effect of size fluctuation on the resonant tunneling characteristics in nanodots arrays through the induced electron energy level disorder. The resonant peak number and peak to valley ratio are found to be closely related

with the degree of disorder and spatial configuration in nanodots. The revealed interesting phenomena provide a theoretical basis for unambiguously experimental exploration of the resonant tunneling information of the electron levels in complicated nanodots arrays.

Acknowledgements This work was supported in part by the Natural Science Foundation of China under the contract of 10125416, and the Shanghai Major Projects of 03DJ14003 and 05DJ14003.

References

[1] D. C. Ralph, C. T. Black, and M. Tinkham, Phys. Rev. Lett. **78**, 4087 (1997).
[2] S. M. Cronenwett, T. H. Oosterkamp, and L. P. Kouwenhoven, Science **281**, 540 (1998).
[3] B. Wang, K. Wang, W. Lu, J. L. Yang, and J. G. Hou, Phys. Rev. B **70**, 205411 (2004).
[4] J. C. Blakesley, P. See, A. J. Shields, B. E. Kardynal, P. Atkinson, I. Farrer, and D. A. Ritchie, Phys. Rev. Lett. **96**, 067401 (2005).
[5] M. A. Reed, J. N. Randall, R. J. Aggarwal, R. J. Matyi, T. M. Moore, and A. E. Wetsel, Phys. Rev. Lett. **60**, 535 (1988).
[6] X. Y. Chen and W. Z. Shen, Appl. Phys. Lett. **85**, 287 (2004).
[7] M. R. Wegewijs and Y. V. Nazarov, Phys. Rev. B **60**, 14318 (1999).
[8] A. S. Alexandrov, A. M. Bratkovsky, and R. S. Williams, Phys. Rev. B **67**, 075301 (2003).
[9] D. M. T. Kuo and Y. C. Chang, Phys. Rev. B **66**, 085311 (2002).
[10] M. Sumetskii, Phys. Rev. B **48**, 14288 (1993).
[11] L. P. Kouwenhoven, Science **268**, 1440 (1995).
L. P. Kouwenhoven, F. W. J. Hekking, B. J. van Wees, C. J. P. M. Harmans, C. E. Timmering, and C. T. Foxon, Phys. Rev. Lett. **65**, 361 (1990).
[12] J. L. Gray, R. Hull, C. H. Lam, P. Sutter, J. Means, and J. A. Floro, Phys. Rev. B **72**, 155323 (2005).
[13] J. M. Garcia, G. Medeiros-Ribeiro, K. Schmidt, T. Ngo, J. L. Feng, A. Lorke, and J. Kotthaus, Appl. Phys. Lett. **71**, 2014 (1997).
[14] J. R. R. Bortoleto, H. R. Gutiérrez, M. A. Cotta, and J. Bettini, Appl. Phys. Lett. **87**, 013105 (2005).
[15] Z. Yu, T. Heinzel, and A. T. Johnson, Phys. Rev. B **55**, 13697 (1997).
[16] R. Ugajin, Phys. Rev. B **59**, 4952 (1999).
[17] C. Flindt, T. Novotny, and A. P. Jauho, Phys. Rev. B **70**, 205334 (2004).
[18] A. Wacker and B. Y. K. Hu, Phys. Rev. B **60**, 16039 (1999).
[19] M. N. Lin, M. T. Lin, C. Y. Liu, M. Y. Lai, N. W. Liu, C. Y. Peng, H. H. Wang, and Y. L. Wang, Appl. Phys. Lett. **87**, 173116 (2005).
[20] M. N. Islam, A. Pradhan, and S. Kumar, J. Appl. Phys. **98**, 024309 (2005).
[21] X. H. Tang, Z. Y. Yin, J. H. Zhao, and S. Deny, Nanotechnology **17**, 295 (2006).
[22] Y. B. Yu, T. C. A. Yeung, W. Z. Shangguan, and C. H. Kam, J. Phys.: Condens. Matter **14**, 703 (2002).
[23] H. Sprekeler, G. Kießlich, A. Wacker, and E. Schöll, Phys. Rev. B **69**, 125328 (2004).
[24] G. Kießlich, A. Wacker, and E. Schöll, Physica B **314**, 459 (2002).
[25] G. Kießlich, A. Wacker, and E. Schöll, Physica E **12**, 837 (2002).
[26] M. Sumetskii, J. Phys.: Condens. Matter **3**, 2651 (1991); Phys. Rev. B **48**, 4586 (1993).
[27] M. Büttiker, Phys. Rev. Lett. **57**, 1761 (1986).
[28] F. Prengel, A. Wacker, and E. Schöll, Phys. Rev. B **50**, 1705 (1994).
[29] Y. Suda and H. Koyama, Appl. Phys. Lett. **79**, 2273 (2001).
[30] R. Duschl, O. G. Schmidt, and K. Eberl, Appl. Phys. Lett. **76**, 879 (2000).

